Neutron-induced fission cross section of ^{232}Th from 1 eV to 20 keV

Yoshihiro Nakagome
Research Reactor Institute, Kyoto University, Kumatori-cho, Sennan-gun, Osaka 590-04, Japan

Robert C. Block and Rudolf E. Slovacek
Department of Nuclear Engineering and Engineering Physics, Rensselaer Polytechnic Institute, Troy, New York 12180

Edgar B. Bean
Knolls Atomic Power Laboratory, Schenectady, New York 12301
(Received 19 November 1990)

The neutron-induced fission cross section of ^{232}Th has been measured from 1 eV to 20 keV using a lead slowing time spectrometer. The cross section was normalized to the ^{238}U(n,f) subthreshold cross section. In the energy region between 1 and 500 eV the fission cross section has a $1/v$ shape, and has a small peak near 5 keV. By extrapolation of $1/v$ the thermal fission cross section of 54 ± 6 μb was deduced. The observed $1/v$ and small-peaked cross sections were interpreted as the fission through the vibrational states in the second well of a triple-humped fission barrier of ^{233}Th.

I. INTRODUCTION

The structure found in the near-threshold and subthreshold fission cross section for heavy actinides has been successfully explained by a double-humped fission barrier model as vibrational states lying in the second well.[1] In the case of light actinides like thorium and protactinium isotopes, the existence of structure in the fission cross section has also been reported by many authors[2–6] and reviewed by James.[7] To interpret the structures observed in the ^{230}Th and ^{232}Th(n,f) cross sections as undamped vibrational levels by the double-humped barrier model, the inner barrier height is required to be $\approx$6 MeV. However, it is shown theoretically that the inner barrier height is $\approx$4.5 MeV,[8] which is lower than the neutron-binding energy. This is called the thorium anomaly.[9]

In order to resolve the thorium anomaly, Möller and Nix[8] proposed a triple-humped barrier model. They introduced mass-asymmetry deformation and found a shallow well near the top of the outer barrier. This model shows that because of the lower first barrier the second and third barriers correspond to the inner and outer barriers of the double-humped barrier model, respectively. It is very important for elucidation of the thorium anomaly to ascertain whether the first barrier of the triple-humped barrier of ^{233}Th is higher or lower than the neutron-binding energy by experiment. For this the neutron-induced fission cross-section measurement for ^{232}Th is necessary in the lower neutron energy region.

Block *et al.*[11] measured the ^{232}Th(n,f) subthreshold cross section in the neutron energy range between 1 eV and 100 keV, and they reported a weak resonance around 2 keV. Perez *et al.*[12] carried out the ^{232}Th(n,f) cross-section measurement at the neutron energy between 100 eV and 1.6 MeV. They found a near constant cross section between 100 and 600 keV, and suggested the first barrier might be higher than the predicted value. Lynn[13] has discussed qualitatively about this plateau region by using vibrational resonances. However, the information on the fission cross section below 100 eV is insufficient.

The ^{232}Th(n,f) cross section at thermal neutron energy has been measured as 60 ± 20 μb by Korneev *et al.*,[14] 48 ± 6 μb by Neve de Mevergnies *et al.*,[15] and ≤4 μb and ≤2.5 μb by Wagemans *et al.*[16,17] Block *et al.*[11] reported a 95 ± 30-μb extrapolated thermal value. These results appear to fall into two groups: 40–100 μb and ≤4 μb. This discrepancy has not been resolved.

To obtain some information on the triple-humped fission barrier for the compound nucleus ^{233}Th and to resolve the discrepancy for the thermal neutron fission cross section, we have measured the ^{232}Th(n,f) cross section from 1 eV to 20 keV using an intense neutron spectrometer, since this subthreshhold fission cross section is expected to be the order of microbarns.

II. EXPERIMENT

The neutron-induced fission cross-section measurement for ^{232}Th was carried out with the Rensselaer Intense Neutron Spectrometer (RINS) system which consists of a 75-tonne lead slowing time spectrometer coupled to the Rensselaer Polytechnic Institute (RPI) Gaerttner Laboratory electron linac. The experimental arrangement is shown in Fig. 1. The RINS system is described in detail in an earlier publication[18] and will only be described briefly here.

The RINS system provides intense neutrons whose flux (per unit energy) $\phi(E)$ in the lead assembly is given[19] by

$$\phi(E)=PE^{-0.776}\exp\left[-\left[\frac{0.2083}{E}\right]^{1/2}\right] \quad (1)$$

and

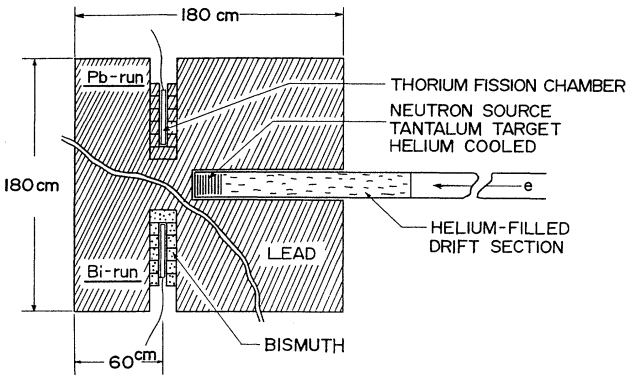

FIG. 1. The experimental arrangements for the measurement of ^{232}Th(n,f) cross section. The electron beam from the linac passes through a thin Ti window and a He-filled drift tube and onto a He-cooled tantalum photonuclear target. The thorium fission chambers are set in the penetration holes placed in the lead assembly. Pb run means the experimental arrangement of the fission chamber surrounded by lead, and Bi run by bismuth.

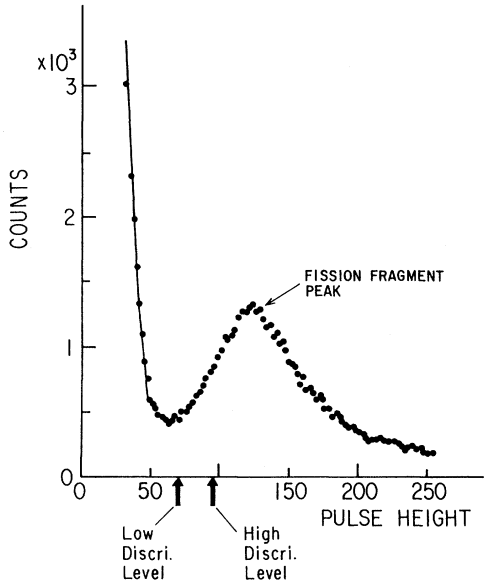

FIG. 2. Pulse-height spectrum of a Th fission chamber. The low- and high-discrimination levels are shown.

$$E=\frac{165\,000}{(t+t_0)^2}\ , \tag{2}$$

where P is a constant that depends on the linac electron power, E is neutron energy (in electron volts) as a function of the slowing-down time t (in microseconds) in the lead assembly, and t_0 is 0.3 μs[18]. The energy resolution at full width at half maximum (FWHM) below 20 keV is represented by the following expression:[20]

$$\left[\frac{\Delta E}{E}\right]_{\text{FWHM}}=\left[0.0746+\frac{0.130}{E}+2.52\times10^{-5}E\right]^{1/2} \tag{3}$$

Four thorium fission chambers were used simultaneously inside the RINS assembly. Each chamber is 2.54-cm diam $\times$ 26.7-cm long and was coated with 210$\pm$1.8 mg of high-purity ^{232}ThO$_2$. The impurities were, in parts per 10^9 (ppb), $\leq$0.04 ppb ^{233}U, $\leq$0.24 ppb ^{234}U, $\leq$25 ppb ^{235}U, $\leq$0.07 ppb ^{236}U, and $\leq$5.2 ppb ^{238}U.

The pulse-height spectrum of each chamber was monitored during the experimental run. In order to check the stability of the electronic circuits and to eliminate electric noise signals, we stored the data by using two different discrimination levels. The high-discrimination level was set at a pulse-height position well above the Th-decay α pulses, but did not cover the whole fission fragment spectrum. The low-discrimination level covered almost the whole fission fragment spectrum but included a part of Th-decay α pulses. The pulse-height spectrum of a Th fission chamber is shown in Fig. 2. The low- and high-discrimination levels are also indicated.

The high- and low-discrimination data were accumulated simultaneously in a computer, and the ratios of these data were determined in certain slowing-down time intervals. The linac was operated at a repetition rate of 400 pulses per second and a pulse width of 66 ns. The power on the photoneutron target was about 1 kW.

We carried out three different experiments for the ^{232}Th(n,f) cross-section measurement. First, the fission events were detected by using the fission chambers surrounded by lead blocks. The distance between each chamber and the tantalum photoneutron target was about 30 cm. The neutron flux was expressed by Eq. (1). Secondly, the chambers were placed in the center of $10\times10\times30$-cm^3 bismuth blocks located inside the RINS assembly as shown in Fig. 1. Bismuth was used to attenuate the high-energy lead capture-gamma rays and thus reduce photofission reactions in the thorium. The neutron-binding energy of bismuth, 4.598 MeV, is below the photofission threshold of ^{232}Th, and the bismuth reduced the high-energy lead capture-gamma-ray intensity to 9.6% of its unshielded value. This quantity of the gamma-ray reduction was calculated numerically for the bismuth blocks used. The neutron flux inside the bismuth blocks was measured by using a highly depleted uranium fission chamber and determined by comparing the fission counting rate with that measured inside lead.

Lastly, we measured the contribution of aluminum capture-induced photofission for ^{232}Th since the fission chambers were made from aluminum whose neutron-binding energy, 7.725 MeV, is well above the photofission threshold of ^{232}Th(γ,f). A fission chamber covered with an aluminum tube with a wall thickness of 0.325 cm placed inside the RINS assembly. This additional aluminum doubled the intensity of Al capture-gamma rays inside the chamber. Then, the contribution of Al capture-induced photofission for ^{232}Th was obtained by subtract-

ing these data from each other.

Fission cross-section data were normalized to the $^{238}U(n,f)$ subthreshold cross section which was measured by Slovacek *et al.*[18] in the energy region between 1 eV and 100 keV using the RINS system. A ^{238}U (4.1±1.4 ppm ^{235}U) fission chamber was used simultaneously with the Th chamber.

The fission detection efficiencies were determined by comparing the integrated whole pulse-height distribution with the pulse-height distribution integrated over the discriminator setting. The whole pulse-height distribution was obtained by extrapolating the observed distribution to zero pulse height.

III. DATA REDUCTION

The relation between the fission counting rate and the fission cross section for ^{232}Th is given by

$$C_T(E)dE = N_T \eta_T k \phi(E) \sigma_T(E) dE \quad \text{inside lead blocks} \tag{4}$$

or

$$C'_T(E)dE = N_T \eta'_T k' \phi'(E) \sigma'_T(E) dE \quad \text{inside bismuth blocks} , \tag{5}$$

where $C_T(E)$, $C'_T(E)$ are the fission counting rates per unit energy at neutron energy E after deadtime and background correction, dE is the neutron energy span corresponding to a given slowing-down time channel, N_T is the number of ^{232}Th atoms in the fission chamber, η_T, η'_T are the fission detection efficiencies in the chamber, k, k' are the flux normalization factors, $\phi(E), \phi'(E)$ are unnormalized neutron flux per unit energy at E, and $\sigma_T(E), \sigma'_T(E)$ are fission cross sections at E for ^{232}Th.

The flux normalization factor k was determined by measuring the $^{238}U(n,f)$ counting rate in a highly depleted uranium (DU) fission chamber inside lead blocks and using the subthreshold fission cross-section resonances at 720 and 1210 eV, which were measured with the RINS system by Slovacek *et al.*[18] Using the equation

$$C_8(E)dE = N_8 \eta_8 k \phi(E) \sigma_8(E) dE , \tag{6}$$

k is given by

$$k = \frac{\int_{400\ \mathrm{eV}}^{3000\ \mathrm{eV}} C_8(E)dE}{N_8 \eta_8 \int_{400\ \mathrm{eV}}^{3000\ \mathrm{eV}} \phi(E) \sigma_8(E) dE} , \tag{7}$$

where $C_8(E)$ is the $^{238}U(n,f)$ counting rate per unit energy at E after deadtime and background correction, N_8 is the number of ^{238}U atoms in the DU chamber, $\eta_8(E)$ is the fission detection efficiency in the chamber, and $\sigma_8(E)$ is the $^{238}U(n,f)$ cross section at E. The integral energy range was selected to include the two ^{238}U subthreshold fission resonances mentioned above.

The neutron flux inside the bismuth blocks, $k'\phi'(E)$, is given by

$$k'\phi'(E)\sigma_8(E)dE = \frac{1}{N_8 \eta'_8} C'_8(E)dE , \tag{8}$$

where $C'_8(E)$ and η'_8 are the quantities measured in a DU fission chamber inside bismuth blocks. In this experiment the shape of the relative neutron flux $\phi'(E)$ was measured and found to be the same as $\phi(E)$ to within ±3.9% from 1eV to 100 keV. Assuming $\phi'(E)=\phi(E)$ and combining with Eq. (6), k' is obtained as follows:

$$k' = k \frac{\eta_8 \int_{1\ \mathrm{eV}}^{150\ \mathrm{eV}} C'_8(E)dE}{\eta'_8 \int_{1\ \mathrm{eV}}^{150\ \mathrm{eV}} C_8(E)dE} . \tag{9}$$

Since the total cross section of bismuth has no structure and is almost constant below 200 eV, the integral energy range was selected as 1 to 150 eV.

IV. EXPERIMENTAL RESULTS

The fission cross-section data for ^{232}Th were juged reliable in the neutron energy region between 1 eV and 20 keV, since the ratio of high- to low-discrimination level data for the bismuth-shielded measurement was constant within ±3.6% from 1 eV to 20 keV but changed considerably above 20 keV.

The cross-section results are shown in Fig. 3. The er-

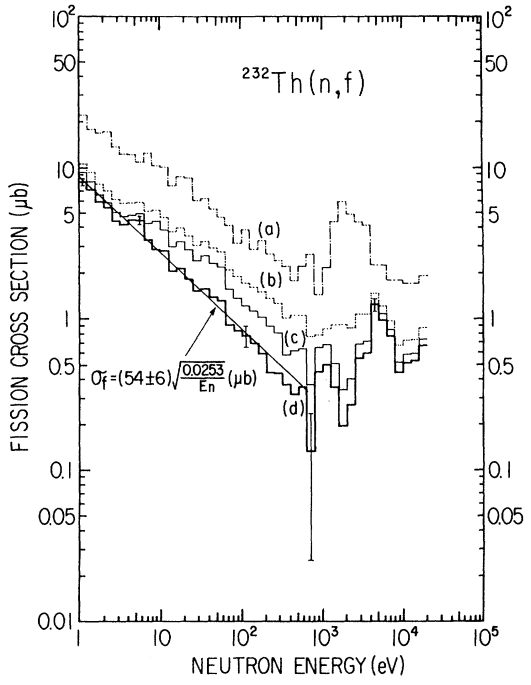

FIG. 3. The fission cross section from 1 eV to 20 keV. (a) The cross section obtained with the thorium fission chambers surrounded by lead; no corrections are applied for photofission; (b) the cross section obtained with the fission chambers surrounded by bismuth shields; no corrections are applied for photofission; (c) the neutron-induced fission cross section in the thorium chambers; corrections have been applied for photofission from lead and aluminum capture; and (d) the $^{232}Th(n,f)$ cross section after correcting for 20 ppb ^{235}U; the straight line is a $1/v$ fit to the data below 500 eV.

rors are 1σ statistical errors from the counting statistics. Figure 3(a) is the result obtained with the chambers surrounded by lead, and Fig. 3(b) is that obtained with the bismuth shielding; no corrections were made for photofission backgrounds. The 6-μb peak near 2 keV in Fig. 3(a), which was reported earlier by Block *et al.*,[11] has disappeared in the cross section of Fig. 3(b). When the bismuth data in Fig. 3(b) are corrected for the 9.6% residual Pb capture-induced photofission and for the photofission from aluminum capture, the results shown in Fig. 3(c) are obtained. The correction of Al capture-induced photofission was 0.29 ± 0.1 μb from 1 to 800 eV and 0.04 ± 0.04 μb above 800 eV. Thus, Fig. 3(c) is the cross section for neutron-induced fission in the fission chamber. A comparison of Figs. 3(a), 3(b), and 3(c) shows that in the energy range from 1 to 100 eV the bismuth shield reduces the net photofission background from 60% (in lead) to 15–25 %.

The neutron-induced fission cross section in Fig. 3(c) appears to fall as $1/v$ from 1 to 4 eV, but then rises above $1/v$ at higher energies. This is attributed to the small amount of ^{235}U in the chamber. Corrections were applied for various amounts of ^{235}U, and a least-squares fit was made relative to a $1/v$ dependence in the 1- to 500-eV energy range. A chi-square minimum was obtained for 20 ppb of ^{235}U; this amount is within the chemical upper limit of 25 ppb ^{235}U. The final ^{232}Th(n,f) cross section corrected for 20 ppb ^{235}U is shown in Fig. 3(d) and listed in Table I. The fission cross section is $1/v$ from 1 to 500 eV and has a 1.2-μb peak near 5 keV. The straight line through the data from 1 to 500 eV is the $1/v$ least-squares fit to the data; the extrapolated thermal fission cross section at 0.0253 eV from this fit is 54 ± 6 μb.

V. ANALYSIS AND DISCUSSION

A. Thermal fission cross section

The 54 ± 6-μb extrapolated thermal fission cross section from this experiment is in good agreement with the 60 ± 20-μb value of Korneev *et al.*[14] and the 48 ± 6-μb value of Neve de Mevergnies *et al.*[15] However, the ≤4-μb and ≤2.5-μb values of Wagemans *et al.*[16,17] are still discrepant with our result. We have estimated the quantity of the thermal neutron fission of ^{233}U which is produced by the neutron capture of ^{232}Th during the experiments. The thorium chambers used in this measurement had little exposure to thermal neutrons and thus produced an upper limit of 1 ppb ^{233}U. This upper limit results in a ≤2.5% reduction of the 54-μb cross section. Thus ^{233}U production is not a principal cause to resolve the present discrepancy.

B. $1/v$ and small-peaked cross section

In order to explain the fission cross section measured in this experiment, we used a triple-humped fission barrier model which was first proposed by Möller and Nix.[8] They predict theoretically that the first innermost barrier height is lower than the neutron-binding energy of ^{232}Th. On the other hand, Perez *et al.*[12] and Lynn[13] suggest that the plateau cross section between 100 and 600 keV, which Perez *et al.* measured, is explained in terms of a damped vibrational state in the second well. This means the first barrier height is very close to the neutron-binding energy. Since our experiment has been carried out in the lower energy region below 100 keV, we support the suggestion of Perez *et al.* in our data analysis.

TABLE I. ^{232}Th(n,f) cross section from 1 eV to 20 keV.

Energy (eV)	σ_f (μb)	Energy (eV)	σ_f (μb)
1.00–1.25	8.07±0.39	158.49–199.52	0.59±0.12
1.25–1.58	7.18±0.34	199.52–251.19	0.44±0.12
1.58–1.99	5.93±0.31	251.19–316.23	0.44±0.11
1.99–2.51	5.41±0.28	316.23–398.11	0.27±0.11
2.51–3.16	4.44±0.26	398.11–501.19	0.31±0.11
3.16–3.98	4.19±0.24	501.19–630.96	0.36±0.11
3.98–5.01	4.48±0.23	630.96–794.33	0.13±0.11
5.01–6.30	4.45±0.23	794.33–1 000.00	0.45±0.06
6.30–7.94	3.30±0.21	1 000.00–1 258.93	0.50±0.06
7.94–10.00	2.85±0.20	1 258.93–1 584.90	0.35±0.07
10.00–12.58	2.79±0.19	1 584.90–1 995.27	0.19±0.07
12.85–15.84	2.05±0.17	1 995.27–2 511.90	0.27±0.06
15.84–19.95	2.14±0.17	2 511.90–3 162.29	0.55±0.09
19.95–25.11	1.82±0.16	3 162.29–3 981.09	0.60±0.09
25.11–31.62	1.52±0.15	3 981.09–5 011.89	1.23±0.10
31.62–39.81	1.57±0.15	5 011.89–6 309.60	0.98±0.09
39.81–50.11	1.39±0.15	6 309.60–7 943.31	0.77±0.08
50.11–63.09	1.31±0.14	7 943.31–10 000.00	0.44±0.07
63.09–79.43	0.91±0.13	10 000.00–12 589.29	0.52±0.07
79.43–100.00	0.84±0.13	12 589.29–15 848.97	0.53±0.07
100.00–125.89	0.77±0.12	15 848.97–19 952.67	0.67±0.07
125.89–158.49	0.69±0.12		

The neutron-induced fission cross section is given by

$$\sigma_{nf}=\sigma_{CN}(E,J)P_f(E)\ , \tag{10}$$

where $\sigma_{CN}(E,J)$ is the formation cross section of compound nucleus at neutron energy E with total angular momentum J, and $P_f(E)$ is the fission probability.

The compound nucleus formation cross section can be written as

$$\sigma_{CN}(E,J)=\pi\lambda\!\!\!^{-}{}_n^{\,2}g_J T_n^l(E)\ , \tag{11}$$

where $\lambda\!\!\!^{-}{}_n$ is the reduced neutron wavelength at E, $g_J=(2J+1)/2(2I+1)$, and T_n^l is the neutron transmission coefficient. T_n^l can be written by using the strength function $\bar{\Gamma}_n^l/\bar{D}$ ($\bar{\Gamma}_n^l/\bar{D}\ll 1$) as follows:

$$T_n^l=1-\exp\left[-\frac{2\pi\bar{\Gamma}_n^l}{\bar{D}}\right]\ , \tag{12}$$

following the method of Moldauer.[21] In our calculation we consider the orbital angular momentum $l=0$ or 1 and use $g_J\bar{\Gamma}_n^0=1.41$ meV, $g_J\bar{\Gamma}_n^1=7.01$ meV, $\bar{D}^0=16.8$ eV, and $\bar{D}^1=15.79$ eV.[10]

As mentioned above, we will now discuss the vibrational states in the second well of the triple-humped barrier (barriers A, B, and C) model. Since the third well has a shallow minimum which is higher than the first barrier height, we can replace the triple-humped barrier by a double-humped barrier (barriers A and B'). For the fission probability, we use the following expression:[22]

$$P_f(E)=\frac{T_i T_o}{(E_{II}-S_n-E)^2(4\pi^2 T'/\bar{D}_{\rm II}^{\,2})+T_i T_o+(T'/4)(T_i+T_0)^2}\ , \tag{13}$$

and

$$T_{i,o}=\frac{1}{1+\exp\left[\dfrac{2\pi(V_{i,o}-S_n-E_n)}{\hbar\omega_{i,o}}\right]}\ , \tag{14}$$

where $V_{i,o}$ are the inner and outer barrier heights, E_{II} the vibrational level in the second well, S_n the neutron-binding energy (4.786 MeV), $\bar{D}_{II}$ the average level spacing in the second well, $\hbar\omega_{i,o}$ the barrier curvatures, and T' is the transmission coefficient for all other decay processes from the compound nucleus. In the calculation of $P_f(E)$, an adequate damping width is taken into account for each vibrational level.

The calculated result of the neutron-induced fission cross section for ^{232}Th below $E\approx 1$ MeV is shown in Fig. 4, and the parameters used are listed in Table II. The correction for RINS energy resolution expressed by Eq. (3) is made below 100 keV. To compare the calculated results with the experimental ones, the other authors' data[5,12] above 10 keV are shown with the present data in Fig. 4. $\bar{D}_{II}=155$ keV is deduced from the experimental data of Perez *et al.*[12] and Behrens *et al.*[3] in the low neutron energy region.

From this calculation, we can understand that the $1/v$ cross section is mainly caused by the damped $\approx$160-keV and $\approx$315-keV ($J=\frac{1}{2}$) vibrational states whose fission widths are 165 μeV and 960 μeV, respectively, and that the small-peaked cross section near 5 keV results from the weak p-wave neutron fission through a nearly pure vibrational state ($J=\frac{3}{2}$, fission width $=28$ μeV) which lies

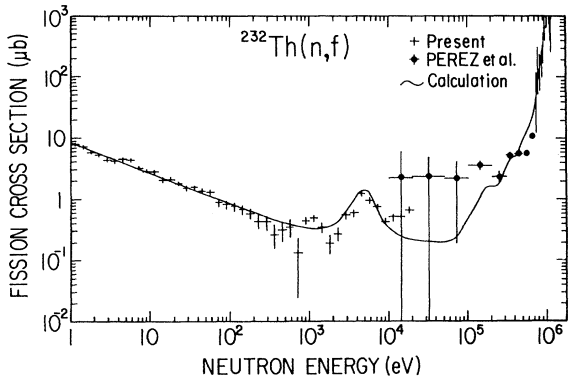

FIG. 4. The calculated and experimental cross sections of the neutron-induced fission of ^{232}Th. The calculation is done below the neutron energy of 1.2 MeV using a double-humped barrier model whose parameters are listed in Table II.

TABLE II. The fission barrier parameters of ^{233}Th for the low-energy region and the vibrational states parameters in the second well.

Barrier parameters		Present
Inner barrier height, V_A (MeV)		5.4
Inner barrier curvature, $\hbar\omega_A$ (MeV)		0.8
Outer barrier height, $V_{B'}$ (MeV)		6.6
Outer barrier curvature, $\hbar\omega_{B'}$ (MeV)		0.55
Average vibrational level spacing in the second well, $\bar{D}_{II}$ (keV)		155
Resonance energy (keV)	J	Damping width (keV)
5	$\frac{3}{2}$	2
160	$\frac{1}{2}$	120
315	$\frac{1}{2}$	150
470	$\frac{3}{2}$	150
625	$\frac{3}{2}$	200
780	$\frac{3}{2}$	80
935	$\frac{1}{2}$	40
1090	$\frac{3}{2}$	100

TABLE III. The fission barrier parameters of ^{233}Th for the high-energy region and the vibrational states parameters in the third well.

Barrier parameters	Present	Blons *et al.*[23]	Caruana *et al.*[4]
Inner barrier height, V_B (MeV)	6.05	6.05	6.2
Inner barrier curvature, $\hbar\omega_B$ (MeV)	1.2	0.4	1.2
Outer barrier height, V_C (MeV)	6.9	6.82	7.0
Outer barrier curvature, $\hbar\omega_C$ (MeV)	1.14	1.14	1.1
Average vibrational level spacing in the third well, $\bar{D}_{III}$ (keV)	155		

Resonance energy (keV)	J	Damping width (keV)
1420	$\frac{1}{2}$	130
1575	$\frac{1}{2}$	80
1730	$\frac{3}{2}$	90
1885	$\frac{3}{2}$	100
2040	$\frac{3}{2}$	100

very close to the neutron-binding energy in the second well. However, we cannot explain the large resonances above ≈ 1.1 MeV, which are measured by Blons *et al.*[5] and Caruana *et al.*,[4] by using our parameters. If we use the parameters listed in Table III in the double-humped barrier (barriers *B* and *C*) calculation, we can almost fit those resonances, but cannot fit the cross sections below ≈ 1.1 MeV. The calculated results are shown in Fig. 5. The barrier and resonance parameters used in the calculations are listed in Tables II and III for the neutron energy below and above ≈ 1.1 MeV, respectively. In Table III the parameters used by the other authors are also listed. These are in good agreement with each other. From the calculations, we can suggest that fission at neutron energies below ≈ 1.1 MeV is caused through the vibrational states in the second well and at above ≈ 1.1 MeV through those in the third well.

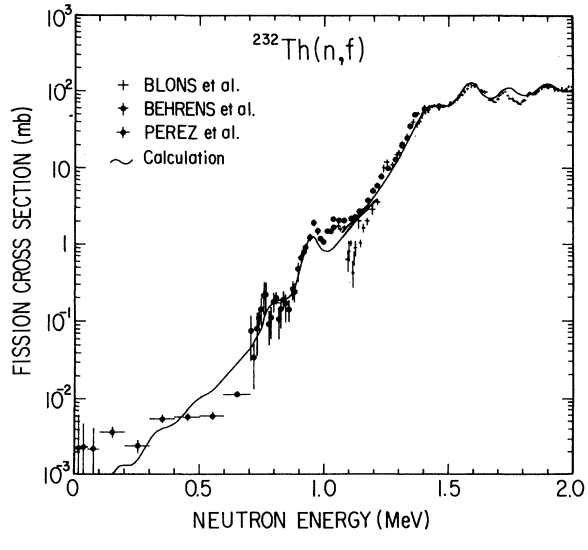

FIG. 5. The same cross sections as in Fig. 3, but magnifying a scale above 100 keV. The calculation below 1.2 MeV uses the parameters listed in Table II, and that above 1.0 MeV uses them listed in Table III.

VI. CONCLUSIONS

The neutron-induced fission cross section cross section of ^{232}Th has been measured from 1 eV to 20 keV using the RINS neutron spectrometer with the neutron slowing-down-time method. The corrections of photofission of ^{232}Th caused by lead and aluminum capture-gamma rays were made experimentally. The $1/v$ cross section was measured in the neutron energy region between 1 and 500 eV, and the thermal neutron fission cross section of 54 ± 6 μb was deduced by extrapolating by $1/v$ to 0.0253 eV. Near 5 keV a small-peaked cross section was measured, whose maximum cross section was about 1.2 μb.

By using a triple-humped barrier model in which the first barrier is higher than the neutron-binding energy, contrary to the theoretical prediction, the $1/v$ cross section is interpreted by the fission through the damped vibrational states in the second well, and the small-peaked cross section near 5 keV is explained as a weak *p*-wave neutron-induced fission through a nearly pure vibrational state ($J=\frac{3}{2}$) in the second well. Further, we can reproduce the fission cross sections in the neutron energy region below about 1.1 MeV by using the same parameters, whereas the fission cross sections at higher neutron energy above 1.1 MeV are interpreted successfully by the fission through the damped vibrational states in the third

well.

Consequently, we understand that the neutron-induced fission cross section of ^{232}Th can be interpreted by the two fission modes, fissions through the damped vibrational states in the second well and in the third well of the triple-humped barrier of ^{233}Th, and that the energy of the third well is about 5.9 MeV.

The present measurement provides information for understanding the fission mode of ^{233}Th.

ACKNOWLEDGMENTS

One of the authors, Y.N., would like to thank Dr. T. Ohsawa of Kinki University and Professor T. Tohei of Tohoku University, Japan for their fruitful discussions about the analysis of the experimental results, and also thank Professor I. Kimura and Professor Y. Fujita of Kyoto University and Professor H. Orihara of Tohoku University, Japan for their continuous encouragement.

[1]V. M. Strutinski, Nucl. Phys. **A95**, 420 (1967).

[2]S. B. Ermagambetov, V. F. Kuzentsov, and G. N. Smirenkin, Yad. Fiz. **5**, 257 (1966) [Sov. J. Nucl. Phys. **5**, 181 (1967)].

[3]J. W. Behrens, J. C. Browne, and E. Ables, Nucl. Sci. Eng. **81**, 512 (1982).

[4]J. Caruana, J. W. Boldeman, and R. L. Walsh, Nucl. Phys. **A285**, 205 (1977).

[5]J. Blons, C. Mazur, D. Paya, M. Ribrag, and H. Weigmann, Nucl. Phys. **A414**, 1 (1984).

[6]S. Plattard, G. F. Auchampaugh, N. W. Hill, G. de Saussure, J. A. Harvey, and R. B. Perez, Phys. Rev. Lett. **46**, 633 (1981).

[7]G. D. James, Radiat. Eff. **92**, 277 (1986).

[8]P. Möller and J. R. Nix, *Physics and Chemistry of Fission* (IAEA, Vienna, 1974), Vol. 1, p. 103.

[9]A. Michaudon, *Nuclear Fission and Neutron-Induced Fission Cross Sections* (Pergamon, Oxford, 1981).

[10]S. F. Mughabghab, *Neutron Cross Sections* (Academic, New York, 1984), Vol. 1, Part B, p. 90-5.

[11]R. C. BLock, J. R. Valentine, R. W. Hockenbury, R. E. Slovacek, E. B. Bean, and D. S. Cramer, in *Proceedings of the International Conference on the Interactions of Neutrons with Nuclei, Lowell, 1976,* CONF-760715-P1, edited by E. Sheldon, G. P. Couchell, S. A. Goodwin, S. C. Mathur, and D. J. Pullen (University of Lowell, Lowell, 1976), Vol. II, p. 1400.

[12]R. B. Perez, G. de Saussure, J. H. Todd, T. J. Yang, and G. F. Auchampaugh, Phys. Rev. C **28**, 1635 (1983).

[13]J. E. Lynn, in *Neutron-Nucleus Collisions—A Probe of Nuclear Structure* (Burr Oak State Park, Glouster, Ohio), Proceedings of the Conference on Neutron-Nuclear Collisions, edited by J. Rapaport, R. W. Finlay, S. M. Grimes, and F. S. Dietrich, AIP Conf. Proc. No. 124 (AIP, New York, 1985), p. 427.

[14]E. I. Korneev, V. S. Skobkin, and G. N. Flerov, Zh. Eksp. Teor. Fiz. **37**, 41 (1960) [Sov. Phys.—JETP **10**, 29 (1960)].

[15]M. Neve de Mevergnies and P. del Marmol, in *Conference on Neutron Cross Sections and Technology,* edited by D. T. Goldman, Natl. Bur. Stand. (U.S.) No. 299, (U.S. GPO, Washington, DC, 1968), Vol. II, p. 611.

[16]C. Wagemans, P. D'Hondt, A. J. Deruytter, A. Emsallem, and M. Asghar, Nucl. Phys. **A259**, 423 (1976).

[17]C. Wagemans, M. Asghar, P. D'Hondt, A. J. Deruytter, and A. Emsallem, Nucl. Phys. **A285**, 32 (1977).

[18]R. E. Slovacek, D. S. Cramer, E. B. Bean, J. R. Valentine, R. W. Hockenbury, and R. C. Block, Nucl. Sci. Eng. **62**, 455 (1977).

[19]H. T. Maguire, Jr., C. R. S. Stopa, R. C. Block, D. R. Harris, R. E. Slovacek, J. W. T. Dabbs, R. J. Dougan, R. W. Hoff, and R. W. Lougheed, Nucl. Sci. Eng. **89**, 293 (1985).

[20]R. C. Little, H. M. Fisher, B. Alam, R. C. Block, D. R. Harris, and R. E. Slovacek, Trans. Am. Nucl. Soc. **53**, 119 (1982).

[21]P. A. Moldauer, Phys. Rev. **157**, 907 (1967).

[22]J. E. Lynn and B. B. Back, J. Phys. A **7**, 395 (1974).

[23]J. Blons, B. Fabro, C. Mazur, D. Paya, M. Ribrag, and Y. Patin, Nucl. Phys. **A477**, 231 (1988).